

## Thermoelastic bending analysis of laminated plates subjected to linear and nonlinear thermal loads

Sandhya K. Swami\*<sup>1</sup> and Yuwaraj M. Ghugal<sup>2a</sup>

<sup>1</sup>Department of Civil Engineering, Marathwada Institute of Technology,  
Aurangabad - 431005, Maharashtra, India

<sup>2</sup>Department of Applied Mechanics, Government College of Engineering,  
Karad-415124, Maharashtra, India

(Received April 5, 2021, Revised July 21, 2021, Accepted July 26, 2021)

**Abstract.** The paper presents the analytical solutions for thick orthotropic laminated plates using trigonometric shear deformation theory. The effects transverse shear and transverse normal strains are included with linear and nonlinear thermal loads. The displacement field of the theory includes the trigonometric functions in thickness coordinate of plate to account for these effects. The displacement field enforces to give the realistic variation of shear stresses across the thickness of plate and thus obviates the need of shear correction factor. The main novelty of the present study is the inclusion of thickness stretching effect in the theory. Another novelty is the application of nonlinear thermal profile consistent with the displacement field of the theory. The principle of virtual work is used to obtain the governing equations and boundary conditions. Simply supported laminated square plates are considered for numerical study to evaluate thermoelastic response. The results obtained by present theory with thickness stretching effect are compared with other refined theories disregarding this effect. It is observed that the results of present theory deviate significantly from the results of other higher order shear deformation theories for antisymmetric crossply laminated plates. The results of symmetric cross-ply laminated plates subjected to linear sinusoidal thermal load are in close agreement with those of exact theory, which validates the accuracy of present shear and normal deformation theory.

**Keywords:** orthotropic plates; principle of virtual work; shear correction factor; thermoelastic analysis

### 1. Introduction

Laminated composites with unidirectional fibers are widely used in aerospace, naval, automobile, sport, and civil engineering and electronics packaging industries due to their high specific strength and high specific stiffness and other superior mechanical and thermal properties. The importance of thermal stresses has been received considerable attention in strength and stability of composite structures made up of laminated plates subjected to severe thermal loadings. A laminated plate consists of orthotropic layers with different fiber orientations. Laminated composite plates may experience thermal deformations due to severe changes in temperature through heating. Failures due to delamination of layers and longitudinal cracks in matrix are the

---

\*Corresponding author, Ph.D., E-mail: mathapatisandhya@gmail.com

<sup>a</sup>Professor, E-mail: ghugal@rediffmail.com

serious problems of laminated structures due to excessive stresses induced by thermal loads at the interfaces between layers. This type of failure is attributed to the large difference in the coefficients of thermal expansion in the direction of fibers and the transverse direction, which develops the high normal stresses in the layers and high shear stresses at the interfaces. Hence, the determination of distribution of these stresses between the layers of laminated composites is highly important in design of composite structures. The aim of the present work is to develop an efficient computational model for thermal analysis of composite laminated plates which includes the effects of both transverse shear and normal stresses. In the literature, different theories and methods of solution exist to assess the flexural behavior of laminated composite plate under various mechanical, thermal, and thermomechanical loadings.

Thermal analysis of thin laminated composite plates by using classical plate theory (CPT) of Kirchhoff (1850) is well known. However, it is inaccurate for multilayered composite plates due to neglect of transverse shear and normal strain effects in the laminate. Mindlin (1951) developed the first order shear deformation theory (FSDT) for elastic plate subjected transverse bending. Since FSDT assumes a constant shear strain across the thickness of plate, it requires problem dependent shear correction factor to appropriately take into account the strain energy of shear deformation. Thermal stresses obtained using classical and first order shear deformation theories are reviewed by Noor and Burton (1992). It has been shown that the classical and first order shear deformation theories are inadequate for predicting the accurate thermal stresses of laminated composite plates. Therefore, various higher order theories have been developed to address the accurate thermal behaviour of laminated composite plates. Comprehensive reviews and comparisons of the accuracy and efficiency of various plate theories are given by Noor and Burton (1989, 1990), Reddy (1993), Carrera (2000), Ghugal and Shimpi (2002), and Sayyad and Ghugal (2015).

Reddy (1984) presented higher order shear deformation theory for flexural analysis of laminated composite plates and Khdeir and Reddy (1991) extended it for thermoelastic flexure of cross-ply laminated plates. Zenkour (2004) studied the static thermo-elastic response of cross-ply laminated plates using a unified shear deformation plate theory without transverse normal effect. Kapania and Mohan (1996) presented the flat shell element for thermal analysis of orthotropic laminated composite plates and shells. Jane and Hong (2000) studied the effect of thermal and mechanical loads on orthotropic plate by using generalized differential quadrature method and explained the effect of thermal expansion force on bending. Cho *et al.* (1989) presented the thermal stress analysis of laminate using layerwise higher-order theory including transverse shear and normal deformation effects.

Yokoo and Matsunaga (1974) and Matsunaga (1992) developed the 2-D theories for elastic shell and plate from 3-D elasticity theory by expanding the displacement field of theory of into power series in thickness coordinate considering the effects of both transverse shear and normal deformations. Matsunaga (2002, 2003) developed the global higher order deformation theories for stress analysis of laminated and sandwich plates under isothermal condition and circular arches subjected to thermal and mechanical loads. Matsunaga (2004, 2005, 2006, 2007a, 2007b) presented global higher order theory for the thermal buckling, buckling and vibration analysis of crossply, angle-ply laminated composite and sandwich plates and cross-ply laminated shallow shells. In these theories, the inplane displacement field consists of ninth order polynomial in global thickness coordinate  $z$ , whereas the transverse displacement consists of an eighth-order in thickness coordinate. Using 2-D global higher order theory, displacements and stresses in simply supported multilayered composite and sandwich plates subjected to thermal loadings are obtained

accurately compared with the exact solutions with small number of unknowns.

Altay and Doekmeçi (2003) reported the usefulness of one- and two-dimensional refined theories of electrostatic structural elements (rods, plates and shells) subjected to coupled mechanical, electrical and thermal effects. Discrepancies with respect to the existence of solutions, convergence, error estimation, and the range of applicability are reported.

Carrera (2000, 2005), Carrera and Ciuffreda (2004), Carrera *et al.* (2013) developed layerwise and equivalent single layer models by using Reissner's mixed variational theorem for evaluating thermal response of orthotropic laminated simply supported plates subjected to constant and linear temperature loadings. Carrera (2005) confirmed the effects of transverse shear and normal strains in thin and thick plates theories while considering temperature profiles that are most important in any refinements of classical and refined plate theories. Carrera *et al.* (2013) presented several hierarchical two-dimensional models, obtained via Carrera's Unified Formulation (CUF), for the thermal stress analysis of multilayered plates and shells. The governing equations are derived using both the principle of virtual displacements and Reissner's mixed variational theorem. Closed form solutions, obtained via the Navier method, are presented for multilayered plates and shells with the assumed and calculated thermal profiles. Kant and Shiyekar (2013) assessed the thermal response of composite laminates using transverse shear and normal deformation theory with twelve unknowns and showed the excellent performance of theory compared with exact thermoelasticity solution. Fares *et al.* (2000) used refined FSDT to evaluate thermal bending of cross ply laminated plates subjected to single sinusoidal linear thermal load. The in-plane displacement field uses sinusoidal function in terms of thickness co-ordinate to include the shear deformation effect. The displacements and stresses for isotropic, orthotropic, two-layer antisymmetric, and three layer symmetric square laminated plates subjected to single sinusoidal and uniformly distributed linear thermal loads and combined uniformly distributed thermo-mechanical loads are obtained by trigonometric shear deformation theory. The transverse displacements of orthotropic and antisymmetric two layer cross-ply laminated plates subjected to non-linear thermal load in combination with transverse mechanical load are presented using trigonometric shear deformation theory for various aspect ratios by Ghugal and Kulkarni (2012). Flexural analysis of nonlinear thermal and mechanical load for symmetric and antisymmetric laminated composite plate are studied by Ghugal and Kulkarni (2012).

Nguyen *et al.* (2016) presented a unified formulation of all higher order shear deformation theories with various polynomial and non-polynomial functions for the analysis of multilayer composite plates considering the transverse normal deformation and developed the new quasi-3D theory which is based on the new transverse shear functions of fifth and seventh order in thickness to involve the normal deformation in the displacement field.

Vekua (1985) has used Legendre's polynomials in terms of thickness coordinate for the expansion of the equations of elasticity and reduction of the 3-D problem to 2-D one and developed the bar, plate, and shell theories. Zhavoronok (2013) presented a new formulation of the Vekua-type  $n$ th order linear theory of thick elastic shells using Lagrange formalism and biorthogonal expansion technique with brief review of construction of general beam, plate, and shell theories. Zozulya (2013, 2015) developed a higher order theory for bars, plates, and thick shells for linear elastic and thermoelastic analyses based on the method developed by Vekua (1985). Ghugal and Kulkarni (2011, 2013) presented the trigonometric shear deformation theory (TSDT) without considering the transverse normal effect across the plate thickness i.e.,  $\varepsilon_z=0$  for isotropic, orthotropic and laminated plates. Bhaskar *et al.* (1996) presented exact elasticity solutions for thermal bending of simply supported composite laminates with which accuracy of

classical and other refined laminate theories can be verified.

Arefi and Amabili (2021) studied the electro-magnetic load effects on the bending and buckling response of doubly curved nanoshell considering thickness stretching effect in total transverse deflection. Arefi and Zenkour (2016) presented thermo-magneto-electro-elastic analysis of a functionally graded nanobeams using sinusoidal shear and normal deformation theory. Arefi *et al.* (2020) studied the effect of thickness stretching on bending response of doubly curved nanoshells using higher order shear deformation theory. Dehsaraji *et al.* (2021) presented the thickness stretching effect which is based on shear and normal deformation theory for functionally graded cylindrical piezoelectric nano/micro shell. Arefi and Arani (2020) presented the analytical solution for simply supported FG nanoplate with piezoelectric effect which is based on four-variable refined plate theory. Arefi and Zenkour (2018) studied free vibration analysis of a three-layered microbeam by using higher order shear deformation theory. Dehsaraji *et al.* (2020) presented vibration analysis of functionally graded nanoshell by using higher-order shear and normal deformation theory to account thickness stretching effect. Dehsaraji *et al.* (2021) studied the buckling response of functionally graded piezoelectric (FGP) cylindrical nanoshell using higher-order shear and normal deformation theory. These studies showed the importance of thickness stretching on the static and dynamic responses of laminated beams, plates and shells under various loading effects.

This paper presents the thermoelastic stress analysis of laminated composite plates including transverse shear and normal deformation effects under linear and non linear thermal loads across the thickness of plate by using trigonometric shear and normal deformation theory. The results obtained by present theory are compared with exact theory for linear thermal load presented by Bhaskar *et al.* (1996). It shows good agreement with exact as well as other refined theories. The novelty of the present study is that it includes the effects of the thickness stretching and the nonlinear thermal profile on the thermoelastic bending response of orthotropic and crossply laminated plates.

## 2. Formulation of the problem

Consider a square cross-ply laminated plate of length  $a$ , width  $b$ , and total thickness  $h$  composed of perfectly bonded orthotropic layers as shown Fig. 1. The material of each layer is assumed to have one plane of material property symmetry parallel to  $x$ - $y$  plane. The coordinate system is such that the mid-plane of the plate coincides with  $x$ - $y$  plane, and  $z$  axis is normal to the

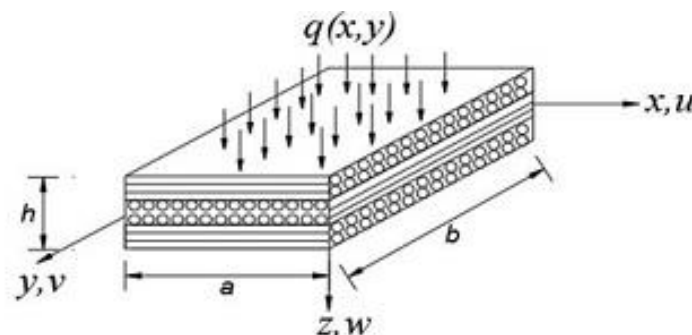


Fig. 1 Plate geometry and coordinate system

middle plane. The upper surface of the plate at  $z=-h/2$  is subjected to a thermal load  $T(x,y,z)$ . The region of the plate in right handed Cartesian coordinate system is

$$0 \leq x \leq a, 0 \leq y \leq b, -h/2 \leq z \leq h/2 \tag{1}$$

Assumptions made in trigonometric shear deformation theory (TSDT)

1. The displacements  $u$ ,  $v$  and  $w$  in  $x$ ,  $y$  and  $z$  directions respectively are small in comparison with the plate thickness and therefore strains are very small. As a result, normal strains  $\epsilon_x$ ,  $\epsilon_y$  and shear strains  $\gamma_{xy}$ ,  $\gamma_{xz}$ ,  $\gamma_{yz}$  can be expressed in terms of displacements  $u$ ,  $v$ , and  $w$  using strain-displacement relations.

2. The transverse displacement  $w$  in  $z$  direction is assumed to be a function of  $x$ ,  $y$  and  $z$ .

3. The body forces are ignored in the analysis.

4. The plate is subjected to linear and nonlinear thermal loads across the thickness of the plate in combination with transverse mechanical load.

5. All layers are perfectly bonded with each other.

6. The functions  $\phi$ ,  $\psi$  and  $\zeta$  are the rotations and are functions of  $x$  and  $y$  only.

### 2.1 The displacement field

The displacement field of the present trigonometric shear and normal deformation theory at a point located at  $(x,y, z)$  in the plate is given by

$$\begin{aligned} u(x, y, z) &= u_0(x, y) - z \frac{\partial w(x, y)}{\partial x} + f(z)\phi(x, y) \\ v(x, y, z) &= v_0(x, y) - z \frac{\partial w(x, y)}{\partial y} + f(z)\psi(x, y) \\ w(x, y, z) &= w(x, y) + g(z)\zeta(x, y) \end{aligned} \tag{2}$$

Here  $u$ ,  $v$  and  $w$  are the unknown displacements of any point in the  $x$ -,  $y$ - and  $z$ - directions, respectively.  $u_0$ ,  $v_0$ ,  $w$  are the unknown displacements of a point on the middle plane in the  $x$ -,  $y$ - and  $z$ -directions, respectively; and  $(\phi, \psi, \zeta)$  are the rotations about  $y$ ,  $x$  and  $z$  axes in  $x$ - $z$ ,  $y$ - $z$  and  $x$ - $y$  planes due to bending. The generalized displacements  $(u_0, v_0, w, \phi, \psi, \zeta)$  are functions of the  $(x, y)$

coordinates and  $f(z) = \frac{h}{\pi} \sin \frac{\pi z}{h}$  and  $g(z) = \cos \frac{\pi z}{h}$  are the transverse shear and normal deformation functions in thickness coordinate  $z$ .

### 2.2 Strain-displacement relationships

The normal and shear strains are obtained within the framework of linear theory of elasticity. The strains associated with the displacement field (2) are as follows,

$$\epsilon_x = \frac{\partial u}{\partial x} = \frac{\partial u_0}{\partial x} - z \frac{\partial^2 w}{\partial x^2} + f(z) \frac{\partial \phi}{\partial x} \tag{3}$$

$$\begin{aligned}
\varepsilon_y &= \frac{\partial v}{\partial y} = \frac{\partial v_0}{\partial y} - z \frac{\partial^2 w}{\partial y^2} + f(z) \frac{\partial \psi}{\partial y} \\
\varepsilon_z &= \frac{\partial w}{\partial z} = -\frac{\pi}{h} \sin\left(\frac{\pi z}{h}\right) \xi \\
\gamma_{xy} &= \frac{\partial u}{\partial y} + \frac{\partial v}{\partial x} = \frac{\partial u_0}{\partial y} + \frac{\partial v_0}{\partial x} - 2z \frac{\partial^2 w}{\partial x \partial y} + f(z) \left( \frac{\partial \phi}{\partial y} + \frac{\partial \psi}{\partial x} \right) \\
\gamma_{xz} &= \frac{\partial u}{\partial z} + \frac{\partial w}{\partial x} = \frac{df(z)}{dz} \left( \phi + \frac{\partial \xi}{\partial x} \right) \\
\gamma_{yz} &= \frac{\partial v}{\partial z} + \frac{\partial w}{\partial y} = \frac{df(z)}{dz} \left( \psi + \frac{\partial \xi}{\partial y} \right)
\end{aligned} \tag{3}$$

### 2.3 Thermoelastic stress-strain relationships

The stress-strain-temperature relationship in  $x, y, z$  coordinate system for the  $k^{\text{th}}$  layer can be written as

$$\begin{Bmatrix} \sigma_x \\ \sigma_y \\ \sigma_z \end{Bmatrix}^k = \begin{bmatrix} Q_{11} & Q_{12} & Q_{13} \\ Q_{12} & Q_{22} & Q_{23} \\ Q_{13} & Q_{23} & Q_{33} \end{bmatrix}^k \begin{Bmatrix} \varepsilon_x - \alpha_x T \\ \varepsilon_y - \alpha_y T \\ \varepsilon_z - \alpha_z T \end{Bmatrix}^k, \quad \tau_{xy} = Q_{66} \gamma_{xy}, \quad \tau_{xz} = Q_{55} \gamma_{xz} \quad \text{and} \quad \tau_{yz} = Q_{44} \gamma_{yz} \tag{4}$$

where lamina reduced stiffnesses for  $k^{\text{th}}$  layer are as follows,

$$\begin{aligned}
Q_{11}^k &= \frac{(1 - \mu_{23}\mu_{32})}{(E_2 E_3 \Delta)}, & Q_{12}^k &= \frac{(\mu_{21} + \mu_{31}\mu_{23})}{(E_2 E_3 \Delta)}, & Q_{13}^k &= \frac{(\mu_{31} + \mu_{21}\mu_{32})}{(E_1 E_3 \Delta)}, & Q_{22}^k &= \frac{(1 - \mu_{13}\mu_{31})}{(E_1 E_3 \Delta)} \\
Q_{23}^k &= \frac{(\mu_{32} + \mu_{12}\mu_{31})}{(E_1 E_3 \Delta)}, & Q_{33}^k &= \frac{(1 - \mu_{12}\mu_{21})}{(E_1 E_2 \Delta)}, & Q_{66}^k &= G_{12}, & Q_{55}^k &= G_{13}, & Q_{44}^k &= G_{23}
\end{aligned} \tag{5}$$

where  $\Delta = (1 - \mu_{12}\mu_{21} - \mu_{23}\mu_{32} - \mu_{31}\mu_{13} - 2\mu_{21}\mu_{32}\mu_{13}) / (E_1 E_2 E_3)$ ,  $E_i$  = elastic moduli,  $G_{ij}$  = shear moduli,  $\mu_{ij}$  = Poisson's ratios, and  $\alpha_x, \alpha_y, \alpha_z$  = coefficients of thermal variation in  $x, y$  and  $z$  directions, respectively.

### 2.4 Temperature field

The variation of constant, linear and non-linear thermal loads across the thickness of plate at a point located at  $(x, y, z)$  in the plate, consistent with the displacement field, is given by,

$$T(x, y, z) = T_0(x, y) + \frac{z}{h} T_1(x, y) + \frac{f(z)}{h} T_2(x, y) = T_z(z) T_\Omega(x, y) \quad \text{and} \quad f(z) = \frac{h}{\pi} \sin \frac{\pi z}{h}$$

where  $T_z(z) = 1, \frac{z}{h}$  and  $\frac{f(z)}{h}$  represent the constant, linear and nonlinear thermal profiles

respectively, across the plate thickness coordinate  $z$ , and  $T_\Omega(x, y)$  represents the temperature distributions over the reference surface  $\Omega$  of the plate.

## 2.5 Governing equations and boundary conditions

Using the expressions for stresses, strains, and principle of virtual work, variationally consistent governing differential equations and boundary conditions for the plate under consideration are obtained. The principle of virtual work applied to the considered plate leads to,

$$\int_{x=0}^a \int_{y=0}^b \int_{z=-\frac{h}{2}}^{\frac{h}{2}} \left[ (\sigma_x \delta \varepsilon_x + \sigma_y \delta \varepsilon_y + \sigma_z \delta \varepsilon_z) + (\tau_{xy} \delta \gamma_{xy} + \tau_{xz} \delta \gamma_{xz} + \tau_{yz} \delta \gamma_{yz}) \right] dx dy dz = \int_{x=0}^a \int_{y=0}^b q(x, y) \delta w dx dy \quad (6)$$

where the symbol  $\delta$  denotes variation of displacement gradients in strains. The axial stress resultants ( $N$ ), moment resultants (stress couples  $M^b$ ), additional stress couples associated with shear deformation effects ( $M^s$ ) and transverse shear stress resultants ( $Q$ ) are introduced as follows:

$$(N_x, N_y, N_{xy}) = \sum_{k=1}^n \int_{z_k}^{z_{k+1}} (\sigma_x, \sigma_y, \tau_{xy}) dz \quad (7)$$

$$(M_x^b, M_y^b, M_{xy}^b) = \sum_{k=1}^n \int_{z_k}^{z_{k+1}} (\sigma_x, \sigma_y, \tau_{xy}) z dz \quad (8)$$

$$(M_x^s, M_y^s, M_{xy}^s) = \sum_{k=1}^n \int_{z_k}^{z_{k+1}} (\sigma_x, \sigma_y, \tau_{xy}) f(z) dz \quad (9)$$

$$(Q_x, Q_y) = \sum_{k=1}^n \int_{z_k}^{z_{k+1}} (\tau_{xz}, \tau_{yz}) g(z) dz \quad (10)$$

$$(Q_z) = \sum_{k=1}^n \int_{z_k}^{z_{k+1}} (\sigma_z) \frac{dg(z)}{dz} dz \quad (11)$$

Here

$$f(z) = \frac{h}{\pi} \sin \frac{\pi z}{h}, \quad g(z) = \frac{df(z)}{dz} = \cos \frac{\pi z}{h} \quad \text{and} \quad \frac{dg(z)}{dz} = -\frac{\pi}{h} \sin \frac{\pi z}{h}$$

Using the stress resultants, Eq. (6) can be written as

$$\int_{x=0}^a \int_{y=0}^b \left\{ \begin{aligned} & \left( N_x \frac{\partial \delta u_0}{\partial x} - M_x^b \frac{\partial^2 \delta w}{\partial x^2} + M_x^s \frac{\partial \delta \varphi}{\partial x} \right) + \left( N_y \frac{\partial \delta v_0}{\partial y} - M_y^b \frac{\partial^2 \delta w_0}{\partial y^2} + M_y^s \frac{\partial \delta \phi}{\partial y} \right) \\ & + \left[ N_{xy} \left( \frac{\partial \delta u_0}{\partial y} + \frac{\partial \delta v_0}{\partial x} \right) - 2M_{xy}^b \frac{\partial^2 \delta w}{\partial x \partial y} + M_{xy}^s \left( \frac{\partial \delta \varphi}{\partial y} + \frac{\partial \delta \phi}{\partial x} \right) \right] \\ & + Q_x \left( \delta \varphi + \frac{\partial \delta \xi}{\partial x} \right) + Q_y \left( \delta \phi + \frac{\partial \delta \xi}{\partial y} \right) + Q_z \delta \xi - q(x, y) \delta w \end{aligned} \right\} dx dy = 0$$

Employing the Green's theorem in this equation successively and collecting the coefficients of  $\delta u_0, \delta v_0, \delta w, \delta \phi, \delta \psi, \delta \xi$  and using the fundamental lemma of the calculus of variations we can obtain the governing equations in terms of force and moment resultants of laminated plate as follows:

$$\delta u_0: \frac{\partial N_x}{\partial x} + \frac{\partial N_{xy}}{\partial y} = 0 \quad (12)$$

$$\delta v_0: \frac{\partial N_y}{\partial y} + \frac{\partial N_{xy}}{\partial x} = 0 \quad (13)$$

$$\delta v_0: \frac{\partial N_y}{\partial y} + \frac{\partial N_{xy}}{\partial x} = 0 \quad (13)$$

$$\delta w: \frac{\partial^2 M_x^b}{\partial x^2} + 2 \frac{\partial^2 M_{xy}^b}{\partial x \partial y} + \frac{\partial^2 M_y^b}{\partial y^2} = q \quad (14)$$

$$\delta \phi: \frac{\partial M_x^s}{\partial x} + \frac{\partial M_{xy}^s}{\partial y} - Q_x = 0 \quad (15)$$

$$\delta \psi: \frac{\partial M_y^s}{\partial y} + \frac{\partial M_{xy}^s}{\partial x} - Q_y = 0 \quad (16)$$

$$\delta \xi: \frac{\partial Q_x}{\partial x} + \frac{\partial Q_y}{\partial y} - Q_z = 0 \quad (17)$$

The associated boundary conditions are obtain in the following form,

Along  $x = 0$  and  $x = a$

Either  $N_x = 0$  or  $u_0$  is prescribed;

Either  $N_{xy} = 0$  or  $v_0$  is prescribed;

Either  $V_x = 0$  or  $w$  is prescribed;

Either  $M_x^b = 0$  or  $\frac{\partial w}{\partial x}$  is prescribed;

Either  $M_x^s = 0$  or  $\phi$  is prescribed;

Either  $M_{xy}^s = 0$  or  $\psi$  is prescribed;

Either  $Q_x = 0$  or  $\xi$  is prescribed;

where  $V_x = \frac{\partial M_x^b}{\partial x} + 2 \frac{\partial M_{xy}^b}{\partial y}$

Along  $y = 0$  and  $y = b$

Either  $N_{xy} = 0$  or  $u_0$  is prescribed;

Either  $N_y = 0$  or  $v_0$  is prescribed;

Either  $V_y = 0$  or  $w$  is prescribed;

Either  $M_y^b = 0$  or  $\frac{\partial w}{\partial y}$  is prescribed;

Either  $M_{xy}^s = 0$  or  $\phi$  is prescribed;

Either  $M_y^s = 0$  or  $\psi$  is prescribed;

Either  $Q_y = 0$  or  $\xi$  is prescribed;

where  $V_y = \frac{\partial M_y^b}{\partial y} + 2 \frac{\partial M_{xy}^b}{\partial x}$

The solution scheme

Here we concern with the closed-form solutions of simply supported square plates. The assumed analytical solution is in the form of double trigonometric series, which satisfies the governing equations and boundary conditions exactly. This type of solution was suggested by Navier for the bending problem of simply supported rectangular plate.

Following are the boundary conditions used for simply supported laminated composite plates along the edges  $x = 0$  and  $x = a$ :

$$N_x = 0, \quad N_{xy} = 0, \quad w_0 = 0, \quad M_x^b = 0, \quad M_x^s = 0, \quad M_{xy}^s = 0, \quad \xi = 0$$

Along the edges  $y = 0$  and  $x = b$ :

$$N_y = 0, \quad N_{xy} = 0, \quad w_0 = 0, \quad M_y^b = 0, \quad M_y^s = 0, \quad M_{xy}^s = 0, \quad \xi = 0$$

The following is the solution form for  $u_0(x, y), v_0(x, y), w(x, y), \phi(x, y), \psi(x, y), \xi(x, y)$  that satisfies the boundary conditions of simply supported plate exactly,

$$\begin{Bmatrix} u_0 \\ v_0 \\ w \\ \phi \\ \psi \\ \xi \end{Bmatrix} = \sum_{m=1}^{\infty} \sum_{n=1}^{\infty} \begin{Bmatrix} u_{mn} \cos \alpha x \sin \beta y \\ v_{mn} \sin \alpha x \cos \beta y \\ w_{mn} \sin \alpha x \sin \beta y \\ \phi_{mn} \cos \alpha x \sin \beta y \\ \psi_{mn} \sin \alpha x \cos \beta y \\ \xi_{mn} \sin \alpha x \sin \beta y \end{Bmatrix} \quad (18)$$

where  $u_{mn}, v_{mn}, w_{mn}, \phi_{mn}, \psi_{mn}, \xi_{mn}$  are the unknown coefficients of respective Fourier series and  $m, n$  are the positive integers, and  $\alpha = m\pi/a$  and  $\beta = n\pi/b$ . The thermal and transverse mechanical loads are expanded in double Fourier sine series as

$$\begin{Bmatrix} T_0 \\ T_1 \\ T_2 \\ q \end{Bmatrix} = \begin{Bmatrix} T_{0mn} \\ T_{1mn} \\ T_{2mn} \\ q_{mn} \end{Bmatrix} \sin \alpha x \sin \beta y \quad (19)$$

where  $T_{0mn}, T_{1mn}, T_{2mn}, q_{mn}$  are the unknown coefficients of respective Fourier series. Substitution of Eqs. (18) and (19) into governing Eqs. (12)-(17), when expressed in terms of displacement variables, yields following set of algebraic equations in matrix form,

$$[K]\{\Delta\} = \{F\} \quad (20)$$

where  $[K]$  is the symmetric stiffness matrix of size  $6 \times 6$ ,  $\{\Delta\} = \{u_{mn}, v_{mn}, w_{mn}, \phi_{mn}, \psi_{mn}, \xi_{mn}\}^T$  and  $\{F\}$  is the generalized force vector. The elements of stiffness matrix  $[K]$  for laminated plate are as follows:

$$K_{11} = A_{11}\alpha^2 + A_{66}\beta^2, \quad K_{12} = K_{21} = A_{12}\alpha\beta + A_{66}\alpha\beta, \quad K_{13} = K_{31} = -(B_{12}\alpha\beta^2 + 2B_{66}\alpha\beta^2 + B_{11}\alpha^3), \quad (21)$$

$$\begin{aligned}
K_{14} = K_{41} = C_{11}\alpha^2 + C_{66}\beta^2, \quad K_{15} = K_{51} = C_{12}\alpha\beta + C_{66}\alpha\beta, \quad K_{16} = K_{61} = -D_{13}\alpha, \\
K_{22} = A_{22}\beta^2 + A_{66}\alpha^2, \quad K_{23} = K_{32} = -(B_{12}\alpha^2\beta + 2B_{66}\alpha^2\beta + B_{22}\beta^3), \quad K_{24} = K_{42} = C_{12}\alpha\beta + C_{66}\alpha\beta \\
K_{25} = K_{52} = C_{22}\beta^2 + C_{66}\alpha^2, \quad K_{26} = K_{62} = -D_{23}\beta, \quad K_{33} = E_{11}\alpha^4 + E_{22}\beta^4 + 2E_{12}\alpha^2\beta^2 + 4E_{66}\alpha^2\beta^2, \\
K_{34} = K_{43} = -(F_{11}\alpha^3 + F_{12}\alpha\beta^2 + 2F_{66}\alpha\beta^2), \quad K_{35} = K_{53} = -(F_{22}\beta^3 + F_{12}\alpha^2\beta + 2F_{66}\alpha^2\beta) \\
K_{36} = K_{63} = J_{13}\alpha^2 + J_{23}\beta^2, \quad K_{44} = L_{11}\alpha^2 + L_{66}\beta^2 + R_{55}, \quad K_{45} = K_{54} = L_{12}\alpha\beta + L_{66}\alpha\beta \\
K_{46} = K_{64} = -P_{13}\alpha + R_{55}\alpha, \quad K_{55} = L_{22}\beta^2 + L_{66}\alpha^2 + R_{44}, \quad K_{56} = K_{65} = -P_{23}\beta + R_{44}\beta \\
K_{66} = R_{55}\alpha^2 + R_{44}\beta^2 + S_{33}
\end{aligned} \tag{21}$$

and the elements of generalized force vector  $\{F\}$  are defined as:

$$\begin{aligned}
F_1 &= -T_{0mn}\alpha(A_{11}\alpha_x + A_{12}\alpha_y + A_{13}\alpha_z) - T_{1mn}\alpha(B_{11}\alpha_x + B_{12}\alpha_y + B_{13}\alpha_z) \\
&\quad - T_{2mn}\alpha(C_{11}\alpha_x + C_{12}\alpha_y + C_{13}\alpha_z) \\
F_2 &= -T_{0mn}\alpha(A_{12}\alpha_x + A_{22}\alpha_y + A_{23}\alpha_z) - T_{1mn}\alpha(B_{12}\alpha_x + B_{22}\alpha_y + B_{23}\alpha_z) \\
&\quad - T_{2mn}\alpha(C_{12}\alpha_x + C_{22}\alpha_y + C_{23}\alpha_z) \\
F_3 &= -T_{0mn} \begin{bmatrix} \alpha^2(B_{11}\alpha_x + B_{12}\alpha_y + B_{13}\alpha_z) \\ + \beta^2(B_{12}\alpha_x + B_{22}\alpha_y + B_{23}\alpha_z) \end{bmatrix} - T_{1mn} \begin{bmatrix} \alpha^2(E_{11}\alpha_x + E_{12}\alpha_y + E_{13}\alpha_z) \\ + \beta^2(E_{12}\alpha_x + E_{22}\alpha_y + E_{23}\alpha_z) \end{bmatrix} \\
&\quad - T_{2mn} \begin{bmatrix} \alpha^2(F_{11}\alpha_x + F_{12}\alpha_y + F_{13}\alpha_z) \\ + \beta^2(F_{12}\alpha_x + F_{22}\alpha_y + F_{23}\alpha_z) \end{bmatrix} + q_{mn} \\
F_4 &= -T_{0mn}\alpha(C_{11}\alpha_x + C_{12}\alpha_y + C_{13}\alpha_z) - T_{1mn}\alpha(F_{11}\alpha_x + F_{12}\alpha_y + F_{13}\alpha_z) \\
&\quad - T_{2mn}\alpha(L_{11}\alpha_x + L_{12}\alpha_y + L_{13}\alpha_z) \\
F_5 &= -T_{0mn}\alpha(C_{12}\alpha_x + C_{22}\alpha_y + C_{23}\alpha_z) - T_{1mn}\alpha(F_{12}\alpha_x + F_{22}\alpha_y + F_{23}\alpha_z) \\
&\quad - T_{2mn}\alpha(L_{12}\alpha_x + L_{22}\alpha_y + L_{23}\alpha_z) \\
F_6 &= T_{0mn}(D_{13}\alpha_x + D_{23}\alpha_y + D_{33}\alpha_z) + T_{1mn}(J_{13}\alpha_x + J_{23}\alpha_y + J_{33}\alpha_z) \\
&\quad + T_{2mn}(P_{13}\alpha_x + P_{23}\alpha_y + P_{33}\alpha_z)
\end{aligned} \tag{22}$$

where  $\alpha_x$ ,  $\alpha_y$  and  $\alpha_z$  are temperature coefficients in  $x$ ,  $y$  and  $z$  directions respectively. The laminates stiffness coefficients  $A_{ij}, B_{ij}, \dots, (i, j = 1, 2, \dots, 6)$  etc. appeared in Eqs. (21) and (22) are defined in terms of reduced stiffness coefficients  $Q_{ij}$  for the  $k$ th layer as follows,

$$A_{ij} = \int_{z=k}^{z=k+1} Q_{ij}^k dz, \quad B_{ij} = \int_{z=k}^{z=k+1} Q_{ij}^k z dz, \quad C_{ij} = \int_{z=k}^{z=k+1} Q_{ij}^k f(z) dz, \quad D_{ij} = \int_{z=k}^{z=k+1} Q_{ij}^k \frac{dg(z)}{dz} dz \tag{23}$$

$$\begin{aligned}
 E_{ij} &= \int_{z=k}^{z=k+1} Q_{ij}^k z^2 dz, & F_{ij} &= \int_{z=k}^{z=k+1} Q_{ij}^k z f(z) dz, & J_{ij} &= \int_{z=k}^{z=k+1} Q_{ij}^k z \frac{dg(z)}{dz} dz \\
 L_{ij} &= \int_{z=k}^{z=k+1} Q_{ij}^k f(z) f(z) dz, & P_{ij} &= \int_{z=k}^{z=k+1} Q_{ij}^k \frac{dg(z)}{dz} f(z) dz, & S_{ij} &= \int_{z=k}^{z=k+1} Q_{ij}^k \frac{dg(z)}{dz} \frac{dg(z)}{dz} dz \\
 R_{ij} &= \int_{z=k}^{z=k+1} Q_{ij}^k g(z) g(z) dz
 \end{aligned} \quad (23)$$

From the solution of Eq. (20) unknown coefficients  $\{\Delta\}$  can be readily obtained with which one can then calculate all the thermal displacements and stresses within the plate.

### 3. Illustrative examples

To assess the performance of present theory, four examples of simply supported laminated square plate subjected to single sinusoidal linear and nonlinear thermal loads through the thickness of plate are considered herein to evaluate the thermal response in the form of displacements and stresses. The linear and nonlinear sinusoidal thermal loads are given by  $T(x, y, z) = zT_1(x, y)$ , and  $f(z)T_2(x, y)$  respectively, with  $m = n = 1$  and  $T_{1mn} = T_{2mn} = \bar{T}_0$ , where  $\bar{T}_0$  is the temperature intensity and  $T_0 = q = 0$  in Eq. (19). The material properties used are as follows:

Material I:  $\frac{E_1}{E_2} = 25, \mu_{12} = 0.25, \frac{\alpha_y}{\alpha_x} = \frac{\alpha_z}{\alpha_x} = 3, G_{12} = G_{13} = 0.5E_2, G_{23} = 0.2E_2, \mu_{21} = \frac{E_2}{E_1} \mu_{12}$

Material II:  $\frac{E_1}{E_2} = 25, \mu_{12} = 0.25, \frac{\alpha_y}{\alpha_x} = \frac{\alpha_z}{\alpha_x} = 1125, G_{12} = G_{13} = 0.5E_2, G_{23} = 0.2E_2, \mu_{21} = \frac{E_2}{E_1} \mu_{12}$

**Example 1:** A simply supported square orthotropic plate subjected to single sinusoidal nonlinear thermal load through the thickness of plate. Material I is used in this problem.

**Example 2:** A simply supported two layer antisymmetric (0<sup>0</sup>/90<sup>0</sup>) square laminated plate subjected to single sinusoidal nonlinear thermal load across the thickness of plate. Material I is used.

**Example 3:** A simply supported square three layer symmetric (0<sup>0</sup>/90<sup>0</sup>/0<sup>0</sup>) cross ply laminated plate subjected to single sinusoidal nonlinear thermal load across the thickness of plate. Material I is used.

**Example 4:** A simply supported square three layer symmetric (0<sup>0</sup>/90<sup>0</sup>/0<sup>0</sup>) cross ply laminated plate subjected to single sinusoidal linear thermal load  $T(x, y, z) = zT_1(x, y)$  across the thickness of plate. Material II is used in this problem.

Following normalized forms are used to present the results of displacements and stresses.

$$\bar{u}\left(0, \frac{b}{2}, -\frac{h}{2}\right) = \frac{u}{\alpha_x \bar{T}_0 a}, \quad \bar{v}\left(\frac{a}{2}, 0, -\frac{h}{2}\right) = \frac{v}{\alpha_x \bar{T}_0 a}, \quad \bar{w}\left(\frac{a}{2}, \frac{b}{2}, 0\right) = \frac{10wh}{\alpha_x \bar{T}_0 a^2} \quad (24)$$

$$\begin{aligned}\bar{\sigma}_x\left(\frac{a}{2}, \frac{b}{2}, -\frac{h}{2}\right) &= \frac{\sigma_x}{\alpha_x \bar{T}_0 E_2 a}, \quad \bar{\sigma}_y\left(\frac{a}{2}, \frac{b}{2}, -\frac{h}{2}\right) = \frac{\sigma_y}{\alpha_x \bar{T}_0 E_2 a}, \quad \bar{\tau}_{xy}\left(0, 0, -\frac{h}{2}\right) = \frac{\tau_{xy}}{\alpha_x \bar{T}_0 E_2 a} \\ \bar{\tau}_{xz}\left(0, \frac{b}{2}, z\right) &= \frac{\tau_{xz}}{\alpha_x \bar{T}_0 E_2 a}, \quad \bar{\tau}_{yz}\left(\frac{a}{2}, 0, z\right) = \frac{\tau_{yz}}{\alpha_x \bar{T}_0 E_2 a}\end{aligned}\quad (24)$$

The transverse shear stresses are evaluated from 3D stress equilibrium equations of theory of elasticity neglecting the body forces. These equations are as follows:

$$\frac{\partial \sigma_x}{\partial x} + \frac{\partial \tau_{xy}}{\partial y} + \frac{\partial \tau_{xz}}{\partial z} = 0, \quad \frac{\partial \tau_{xy}}{\partial x} + \frac{\partial \sigma_y}{\partial y} + \frac{\partial \tau_{yz}}{\partial z} = 0 \quad (25)$$

#### 4. Numerical results and discussion

The numerical results for thermoelastic bending analysis of simply supported orthotropic, two layer antisymmetric and three layer symmetric cross-ply laminated plates subjected to nonlinear sinusoidal thermal loads are discussed in this section. The results of present theory are compared with those of TSDT of Ghugal and Kulkarni (2013), HSDT of Reddy (1984), FSDT of Mindlin (1951), CPT of Kirchhoff (1850) in which the effect of thickness stretching is neglected. The results of three layer symmetric cross-ply laminated plates subjected to linear sinusoidal thermal load are also presented and compared with the exact theory for linear thermal load presented by Bhaskar *et al.* (1996) to validate the accuracy of present shear and normal deformation theory. The results are presented in numerical and graphical forms in Tables 1 through 4 and in Figs. 1 through 13 for various aspect ratios followed by examplewise discussion emphasizing the effects of thickness stretching and nonlinear thermal profile.

Inplane displacements  $(\bar{u}, \bar{v})$  for orthotropic plate are presented in Table 1 for aspect ratios 4 and

Table 1 Normalized displacements and stresses for square orthotropic plate subjected to single sinusoidal nonlinear thermal load (Example 1)

Theory	$S$	$\bar{u}$	$\bar{v}$	$\bar{w}$	$\bar{\sigma}_x$	$\bar{\sigma}_y$	$\bar{\tau}_{xy}$	$\bar{\tau}_{xz}^{EE}$	$\bar{\tau}_{yz}^{EE}$
Present		0.3092	0.3722	1.7860	1.5182	1.3892	1.0240	0.0186	0.1227
TSDT		0.2844	0.3434	1.8919	1.5424	1.3607	0.9862	0.0066	0.1191
HSDT	4	0.2585	0.3141	1.8504	1.6251	1.4518	0.9423	0.0453	0.1504
FSDT		0.2814	0.3563	1.9279	1.3164	1.3224	1.0018	0.0143	0.1186
CPT		0.2874	0.2874	1.8293	1.7270	1.5349	0.9027	0.0755	0.1798
Present		0.2904	0.3020	1.8407	1.8610	1.5570	0.9340	0.0526	0.0678
TSDT		0.2867	0.3004	1.8464	1.6898	1.4943	0.9223	0.0237	0.0663
HSDT	10	0.2871	0.2874	1.8496	1.7120	1.5018	0.9189	0.0254	0.0674
FSDT		0.2860	0.3032	1.8520	1.6323	1.4859	0.9256	0.0246	0.0663
CPT		0.2874	0.2874	1.8293	1.7270	1.5349	0.9027	0.0302	0.0719

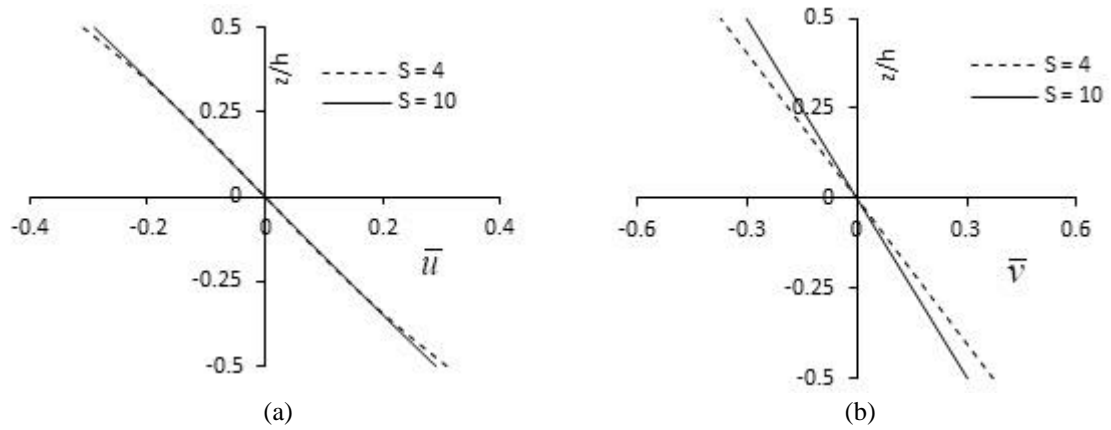


Fig. 2 Variation of normalized inplane displacements ( $\bar{u}$ ,  $\bar{v}$ ) through the thickness of orthotropic plate subjected to single sinusoidal nonlinear thermal load for aspect ratio 4 and 10

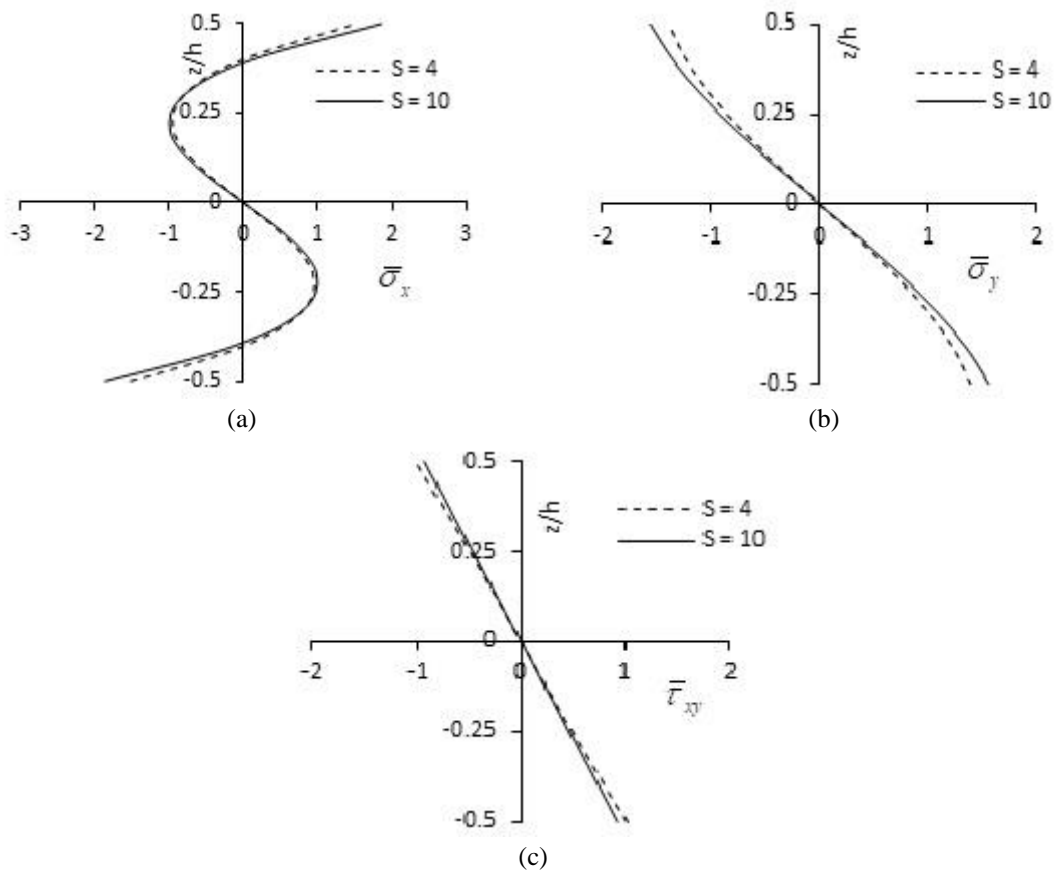


Fig. 3 Variation of normalized inplane stresses ( $\bar{\sigma}_x$ ,  $\bar{\sigma}_y$ ) and inplane shear stresses ( $\bar{\tau}_{xy}$ ) through the thickness of orthotropic plate subjected to single sinusoidal nonlinear thermal load for aspect ratios 4 and 10

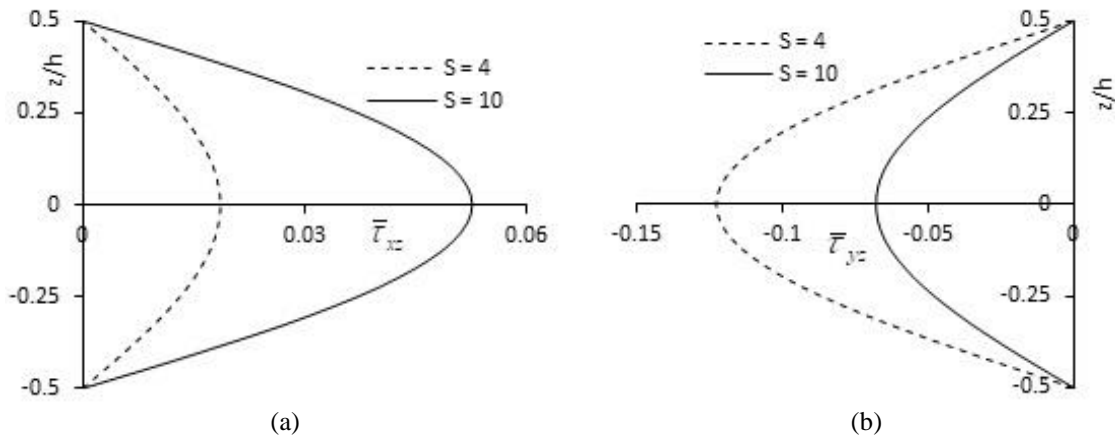


Fig. 4 Variation of normalized transverse shear stresses ( $\bar{\tau}_{xz}$ ,  $\bar{\tau}_{yz}$ ) through the thickness of orthotropic plate subjected to single sinusoidal nonlinear thermal load for aspect ratios 4 and 10

10. Inplane displacement ( $\bar{u}$ ) obtained by present theory are in good agreement with HSDT, FSDT and CPT for side to thickness ratios 4 and 10. Inplane displacement ( $\bar{v}$ ) obtained by present theory is comparable with HSDT, whereas FSDT overpredicts this displacement significantly compared to that of present theory and HSDT, whereas CPT under predicts the displacement ( $\bar{v}$ ) for aspect ratio 4. The difference in inplane displacements in this case is due to the different coefficients of thermal expansions in respective direction. Variation of inplane displacements is shown in Fig. 2 for aspect ratios 4 and 10. Transverse displacement ( $\bar{w}$ ) obtained for orthotropic plate by present theory for aspect ratio 4 is in good agreement with higher order shear deformation theory, whereas FSDT over predicts the transverse displacement for aspect ratio 4. For aspect ratio 10, the results obtained by present theory, HSDT, FSDT and CPT are more or less identical. Inplane normal stress ( $\bar{\sigma}_x$ ) obtained for orthotropic plate by present theory is comparable with HSDT, whereas FSDT underpredicts the normal stress ( $\bar{\sigma}_x$ ) and CPT yields much higher value for aspect ratio 4. For aspect ratio 10, results obtained by present theory are comparable with each other. The through thickness variation of normal stress ( $\bar{\sigma}_x$ ) for orthotropic plate is shown in Fig. 3 indicating the severe effect of thickness stretching and non-linear thermal load for aspect ratios 4 and 10 with change in sign. Inplane normal stress ( $\bar{\sigma}_x$ ) obtained by present theory is comparable with HSDT and FSDT, whereas CPT overpredicts the same for aspect ratios 4 and 10. This stress shows nonlinear variation through the thickness as shown in Fig. 3. Inplane shear stresses obtained by present theory, HSDT, FSDT and CPT are more or less identical. This stress varies linearly through the thickness of orthotropic plate as shown in Fig. 3. Transverse shear stresses ( $\bar{\tau}_{xz}$ ,  $\bar{\tau}_{yz}$ ) obtained by present theory for orthotropic plates are comparable with HSDT and FSDT, whereas CPT overpredicts these stresses for aspect ratio 4. The through the thickness variations of these stresses is shown in Fig. 4 for aspect ratios 4 and 10. The variations of these stresses are different from each other with change in sign due to the distinct transverse shear stiffnesses in  $xz$  and  $yz$  planes of the plate.

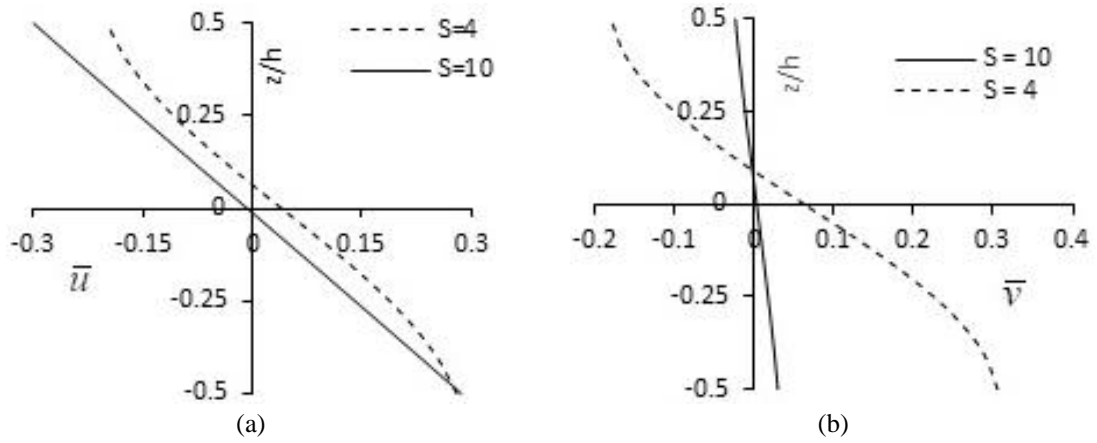


Fig. 5 Variation of normalized inplane displacements ( $\bar{u}$ ,  $\bar{v}$ ) through the thickness of two layer ( $0^0/90^0$ ) laminated plate subjected to nonlinear single sinusoidal thermal load for aspect ratios 4 and 10

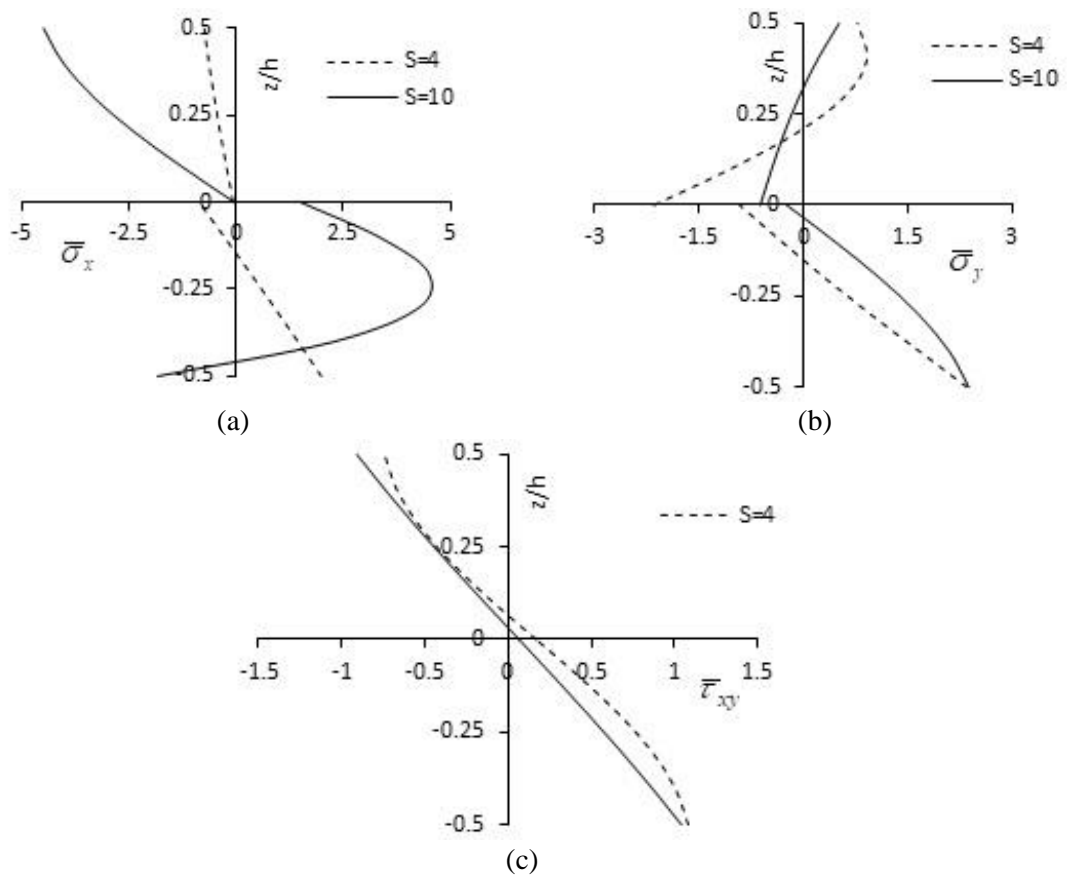


Fig. 6 Variation of normalized inplane stresses ( $\bar{\sigma}_x$ ,  $\bar{\sigma}_y$ ) and inplane shear stresses ( $\bar{\tau}_{xy}$ ) through the thickness of two layer ( $0^0/90^0$ ) laminated plate subjected to nonlinear single sinusoidal thermal load for aspect ratios 4 and 10

Table 2 Normalized displacements and stresses for square two layer (0<sup>0</sup>/90<sup>0</sup>) laminated plate subjected to single sinusoidal nonlinear thermal load (Example 2)

Theory	S	$\bar{u}$	$\bar{v}$	$\bar{w}$	$\bar{\sigma}_x$	$\bar{\sigma}_y$	$\bar{\tau}_{xy}$	$\bar{\tau}_{xz}^{EE}$	$\bar{\tau}_{yz}^{EE}$
Present		0.2799	0.3057	1.8349	1.9856	2.3541	1.0808	0.1412	0.1412
TSDT		0.2914	0.3321	1.9460	2.0811	2.0811	0.9794	0.1246	0.1246
HSDT	4	0.2934	0.3329	2.0156	2.2418	2.2418	0.9839	0.1250	0.1268
FSDT		0.2926	0.3325	1.9899	2.1765	2.1765	0.9820	0.1268	0.1262
CPT		0.2926	0.3325	1.9899	2.1765	2.1765	0.9820	0.1262	0.1262
Present		0.2862	0.2997	1.7488	1.8285	2.3807	1.0408	0.0586	0.0616
TSDT		0.2924	0.3325	1.9827	2.1609	2.1609	0.9816	0.0504	0.0504
HSDT	10	0.2930	0.3327	2.0007	2.2040	2.2040	0.9828	0.0503	0.0506
FSDT		0.2926	0.3325	1.9899	2.1765	2.1765	0.9820	0.0505	0.0505
CPT		0.2926	0.3325	1.9899	2.1765	2.1765	0.9820	0.0505	0.0505

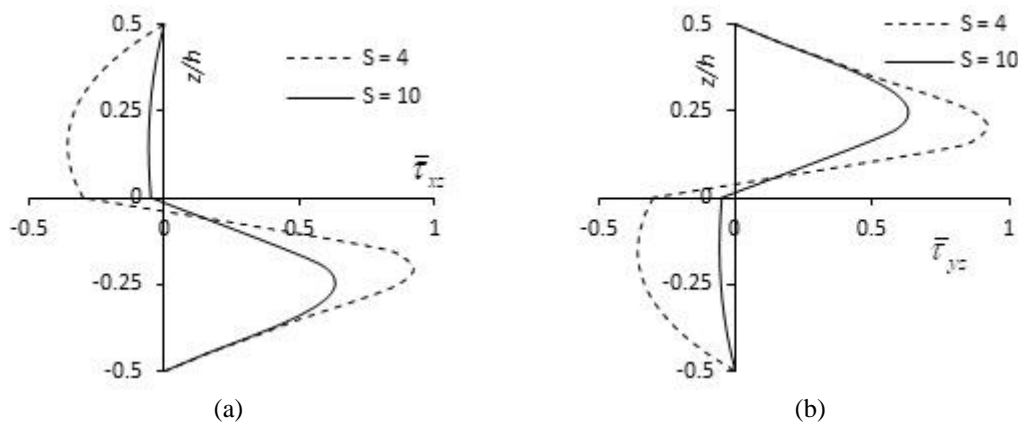


Fig. 7 Variation of normalized transverse shear stresses ( $\bar{\tau}_{xz}$ ,  $\bar{\tau}_{yz}$ ) through the thickness of two layer (0<sup>0</sup>/90<sup>0</sup>) laminated plate subjected to nonlinear single sinusoidal thermal load for aspect ratios 4 and 10

Inplane displacements ( $\bar{u}$ ,  $\bar{v}$ ) for two layer antisymmetric crossply laminated plate are presented in Table 2 for aspect ratios 4 and 10. Inplane displacements obtained by present theory, HSDT, FSDT and CPT are more or less identical with each other for aspect ratios 4 and 10. Variation of inplane displacements is shown in Fig. 5 for aspect ratios 4 and 10. For aspect ratio 4, the variations of these displacements are nonlinear through the thickness showing the shift above the midsurface of the plate due to severe warping and unsymmetry in stacking sequence. Transverse displacements ( $\bar{w}$ ) obtained by present theory are in good agreement with HSDT and FSDT, whereas CPT underestimates the transverse displacement for aspect ratios 4 and 10. Inplane normal stress ( $\bar{\sigma}_x$ ) obtained by present theory is comparable with HSDT, whereas FSDT underpredicts the normal stress ( $\bar{\sigma}_x$ ) and CPT yields much higher value for aspect ratio 4. For aspect ratio 10, results obtained by present theory are comparable with each other. The through thickness variation normal stress ( $\bar{\sigma}_x$ ) is shown in Fig. 6. The variation of this stress is nonlinear in bottom layer and changes

Table 3 Normalized displacements and stresses for square three layer (0<sup>0</sup>/90<sup>0</sup>/0<sup>0</sup>) laminated plate subjected to single sinusoidal nonlinear thermal load (Example 3)

Theory	S	$\bar{u}$	$\bar{v}$	$\bar{w}$	$\bar{\sigma}_x$	$\bar{\sigma}_y$	$\bar{\tau}_{xy}$	$\bar{\tau}_{xz}^{EE}$	$\bar{\tau}_{yz}^{EE}$
Present		0.2980	0.3411	1.8413	1.5672	1.4419	1.0913	0.0224	0.1518
TSDT		0.2855	0.3269	1.9405	1.6163	1.4118	0.9620	0.0384	0.1212
HSDT	4	0.2857	0.3139	1.8803	1.6150	1.4527	0.9417	0.0672	0.1317
FSDT		0.2810	0.3388	1.9463	1.2646	1.3781	0.9734	0.0425	0.1157
CPT		0.2873	0.2873	1.8292	1.7249	1.5350	0.9027	0.1111	0.1559
Present		0.2906	0.3014	1.8550	1.8740	1.5640	0.9300	0.0386	0.0613
TSDT		0.2869	0.2976	1.8599	1.7015	1.5030	0.9189	0.0369	0.0588
HSDT	10	0.2873	0.2977	1.8654	1.7285	1.5025	0.9188	0.0381	0.0588
FSDT		0.2857	0.3001	1.8583	1.6103	1.4960	0.9203	0.0376	0.0584
CPT		0.2873	0.2873	1.8292	1.7249	1.5350	0.9027	0.0445	0.0623

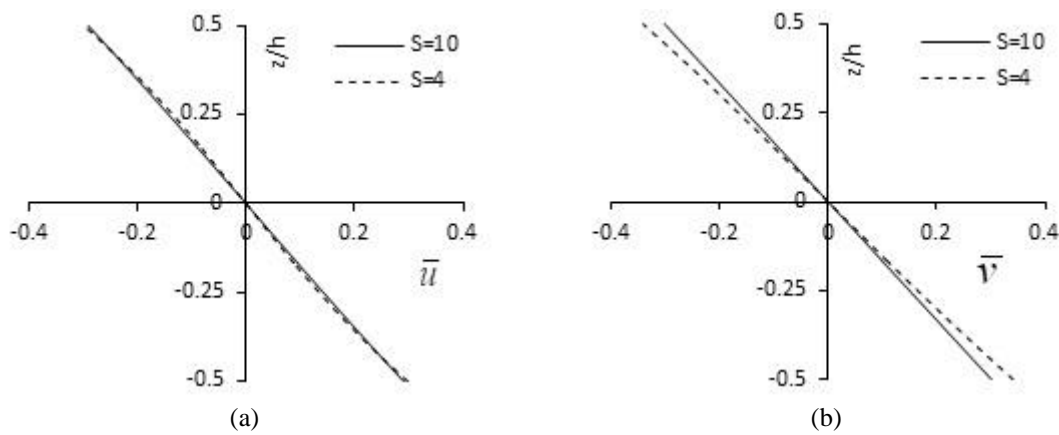


Fig. 8 Variation of normalized inplane displacements ( $\bar{u}$ ,  $\bar{v}$ ) through the thickness of three layer (0<sup>0</sup>/90<sup>0</sup>/0<sup>0</sup>) laminated plate subjected to single sinusoidal nonlinear thermal load for aspect ratios 4 and 10

its sign. Inplane normal stresses ( $\bar{\sigma}_y$ ) obtained by present theory are comparable with HSDT, FSDT, and CPT for both aspect ratios 4 and 10. The through thickness variation ( $\bar{\sigma}_y$ ) for two layer laminated plate is shown in Fig. 6 for aspect ratios 4 and 10 depicting the nonlinear behaviour. Inplane shear stresses ( $\bar{\tau}_{xy}$ ) obtained by present theory, HSDT, HSDT and CPT are more or less identical. This stress shows nonlinear behaviour across the thickness of plate at aspect ratio 4 as shown in Fig. 6. Transverse shear stresses ( $\bar{\tau}_{xz}$ ,  $\bar{\tau}_{yz}$ ) obtained by present theory for unsymmetric laminate are higher than those given by HSDT, FSDT, and CPT for the aspect ratio 4 and for aspect ratio 10, these stresses are closer to each other. Variations of transverse shear stresses through the thickness of unsymmetric laminate is shown in Fig. 7 for aspect ratios 4 and 10. The variations of these stresses are different from each other with change in sign. The reason for deviation in results of displacements and stresses obtained by present theory compared to other

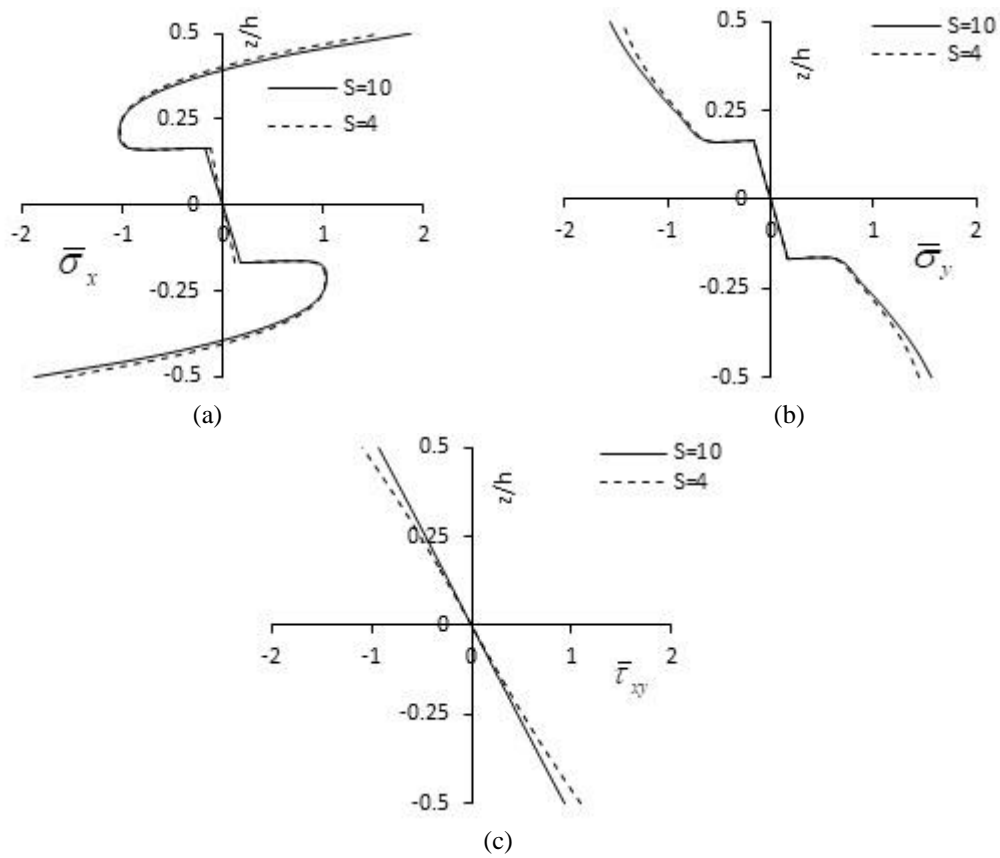


Fig. 9 Variation of normalized inplane stresses ( $\bar{\sigma}_x, \bar{\sigma}_y$ ) and inplane shear stresses ( $\bar{\tau}_{xy}$ ) through the thickness of three layer ( $0^0/90^0/0^0$ ) laminated plate subjected to single sinusoidal nonlinear thermal load for aspect ratios 4 and 10

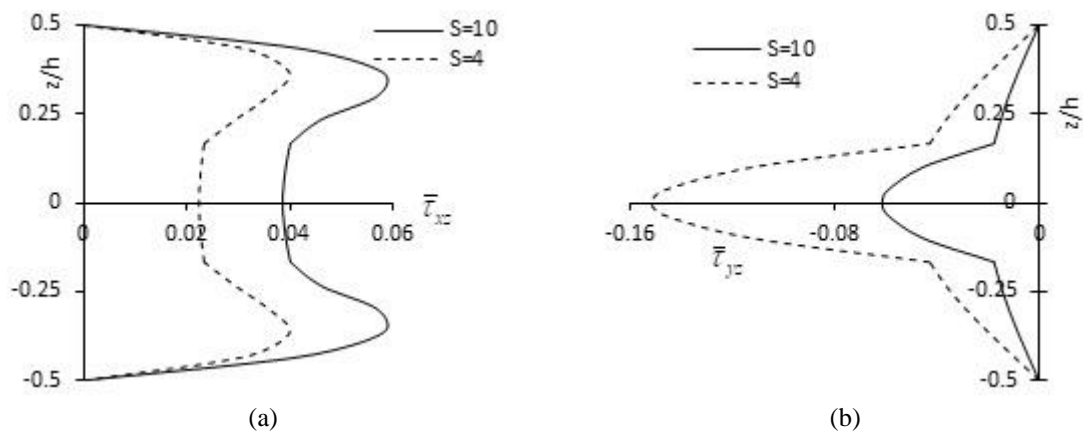


Fig. 10 Variation of normalized transverse shear stresses ( $\bar{\tau}_{xy}, \bar{\tau}_{yz}$ ) through the thickness of three layer ( $0^0/90^0/0^0$ ) laminated plate subjected to non-linear single sinusoidal thermal load for aspect ratios 4 and 10

refined theories is due to the neglect of thickness stretching effect in other theories while

Table 4 Normalized displacements and stresses for square three layer (0<sup>0</sup>/90<sup>0</sup>/0<sup>0</sup>) laminated plate subjected to single sinusoidal linear thermal load (Example 4)

Theory	S	$\bar{u}$	$\bar{v}$	$\bar{w}$	$\bar{\sigma}_x$	$\bar{\sigma}_y$	$\bar{\tau}_{xy}$	$\bar{\tau}_{xz}^{EE}$	$\bar{\tau}_{yz}^{EE}$
Present		20.40	68.03	43.45	1281.70	961.55	138.91	84.11	120.22
HSDT	4	18.17	75.97	42.02	1189.39	871.19	148.11	88.62	136.27
Exact		18.11	81.83	42.69	1183.00	856.10	157.00	84.81	128.70
Present		17.37	29.49	17.57	1002.40	1088.20	73.62	60.59	68.31
HSDT		16.53	30.18	16.89	1020.33	1019.00	73.48	61.71	66.72
FSDT	10	14.55	27.62	12.83	860.50	1029.00	66.24	64.67	67.22
CPT		15.99	15.99	10.18	964.60	1065.00	50.23	70.85	70.85
Exact		16.61	31.95	17.39	1026.00	1014.00	76.29	60.54	66.01
Present		17.02	20.33	12.56	965.09	1024.70	58.69	33.51	35.05
HSDT		16.12	19.81	11.95	979.70	1052.00	56.54	34.17	34.86
FSDT	20	15.60	19.10	10.89	936.70	1055.00	54.52	34.58	34.92
CPT		15.99	15.99	10.18	964.60	1065.00	50.23	35.42	35.42
Exact		16.17	20.34	12.12	982.00	1051.00	57.35	33.98	34.76
Present		16.93	17.47	11.06	954.89	1033.20	54.06	13.81	14.13
HSDT		16.00	16.60	10.46	967.10	1063.00	51.30	14.08	14.13
FSDT	50	15.92	16.50	10.29	960.00	1063.00	50.93	14.10	14.13
CPT		15.99	15.99	10.18	964.60	1065.00	50.23	14.17	14.17
Exact		16.02	16.71	10.50	967.50	1063.00	51.41	14.07	14.13

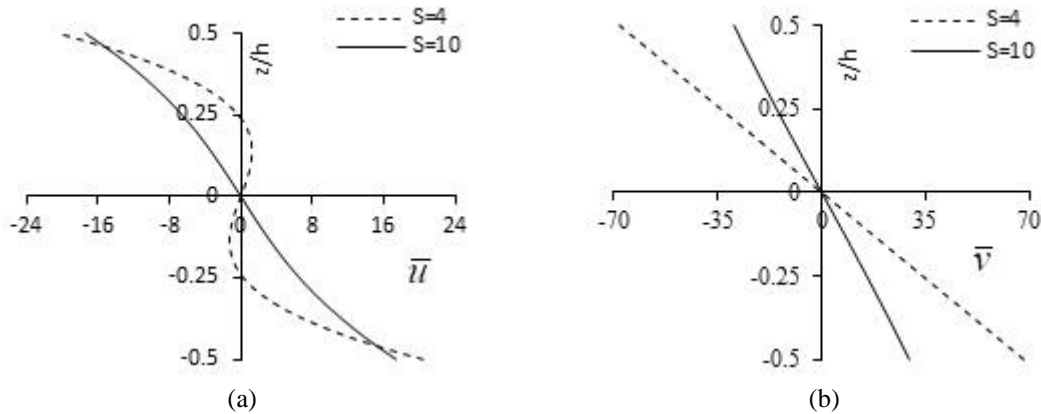


Fig. 11 Variation of normalized inplane displacements ( $\bar{u}, \bar{v}$ ) through the thickness of three layer (0<sup>0</sup>/90<sup>0</sup>/0<sup>0</sup>) laminated plate subjected to single sinusoidal linear thermal load for aspect ratios 4 and 10

subjecting the plates to nonlinear thermal load.

Inplane displacements ( $\bar{u}, \bar{v}$ ) for three layer laminated plate are presented in Table 3 for aspect ratios 4 and 10. Inplane displacements obtained by present theory are higher than those given by TSDT and HSDT without thickness stretching effect, FSDT and CPT for aspect ratios 4 and 10. It is observed that the inplane displacement in the fibre direction is less as compared to that in the

transverse direction. Variations of normalized inplane displacements through the thickness of three layer ( $0^0/90^0/0^0$ ) laminated plate subjected to nonlinear single sinusoidal thermal load for aspect ratios 4 and 10 are shown in Fig. 8. The severe warping of laminate is not observed in this case since the stacking sequence of layers is symmetric. Transverse displacements ( $\bar{w}$ ) obtained by present theory is lower than that is given by TSDT, HSDT and FSDT, and it is higher than that is given by CPT for aspect ratios 4 and 10.

Inplane normal stress ( $\bar{\sigma}_x$ ) obtained by present theory is comparable with TSDT and HSDT, whereas FSDT yields lower value and CPT yields much higher value for aspect ratio 4. For aspect ratio 10, the value of this stress is significantly higher than that is given by other refined theories disregarding thickness stretching effect. The increase in this bending stress with increase in aspect ratio is due to decrease in shear deformation and increase in thickness stretching effect. Similar trend is observed for inplane normal stress ( $\bar{\sigma}_y$ ). The through thickness variations normal stresses ( $\bar{\sigma}_x, \bar{\sigma}_y$ ) obtained by present theory is shown in Fig. 9 indicating severe nonlinearity in top and bottom layers. Inplane shear stresses obtained by present theory are higher than those obtained by TSDT, HSDT, FSDT, and CPT for both the aspect ratios.

Transverse shear stresses ( $\bar{\tau}_{xz}, \bar{\tau}_{yz}$ ) or interlaminar stresses obtained by present theory for symmetric laminate deviate considerably compared to those of TSDT and HSDT disregarding the thickness stretching effect, and FSDT whereas CPT yields much higher values for aspect ratios 4 and 10. The point of maximum shear stress  $\bar{\tau}_{xz}$  is no longer at the neutral plane but is moved towards the extreme fibers. The maximum value of  $\bar{\tau}_{xz}$  occurs at  $z = \pm 3h/8$  from neutral plane in  $0^0$  layers and minimum value occurs at the neutral plane ( $z = 0$ ), whereas the maximum value of  $\bar{\tau}_{yz}$  occurs at the neutral plane of the laminate passing through the  $90^0$  layer. These stresses across the thickness of laminate are responsible for the delamination type failure at the interfaces and the cracking of matrix elsewhere. Variations of transverse shear stresses through the thickness of symmetric laminate are shown in Fig. 10 for aspect ratios 4 and 10. The variations of these stresses are different from each other with change in sign. These stresses vary according to cosine law across the thickness of laminated plate satisfying the zero shear stress conditions at the top and bottom surfaces of the plate and continuity conditions at the interfaces between the layers.

Numerical results for displacements and stresses for square three layer ( $0^0/90^0/0^0$ ) laminated plate subjected to single sinusoidal linear thermal load are presented in Table 4 and in Figs.11 through 13 and discussed with exact theory of Bhaskar *et al.* (1996) and HSDT of Kant and Shiyekar (2013) to verify the accuracy of present theory.

Inplane displacements ( $\bar{u}, \bar{v}$ ) are presented in Table 4 for aspect ratios 4, 10, 20 and 50. The present theory yields values these displacements with reasonable accuracy for very thick laminate compared to those of exact theory and HSDT of Kant and Shiyekar (2013) with twelve unknown variables. For moderately thick plate ( $a/h = 10$ ), the results of present theory are in close agreement with those of HSDT and exact theory, whereas FSDT and CPT underpredict these displacements. For aspect ratios 20 and 50, all the two dimensional theories predict excellent values of these displacements when compared with exact results due decrease in shear deformation. The through thickness variation of inplane displacements  $\bar{u}$  and  $\bar{v}$  are shown in Fig. 11. The variation of inplane displacement  $\bar{u}$  shows the severe warping effect on laminated

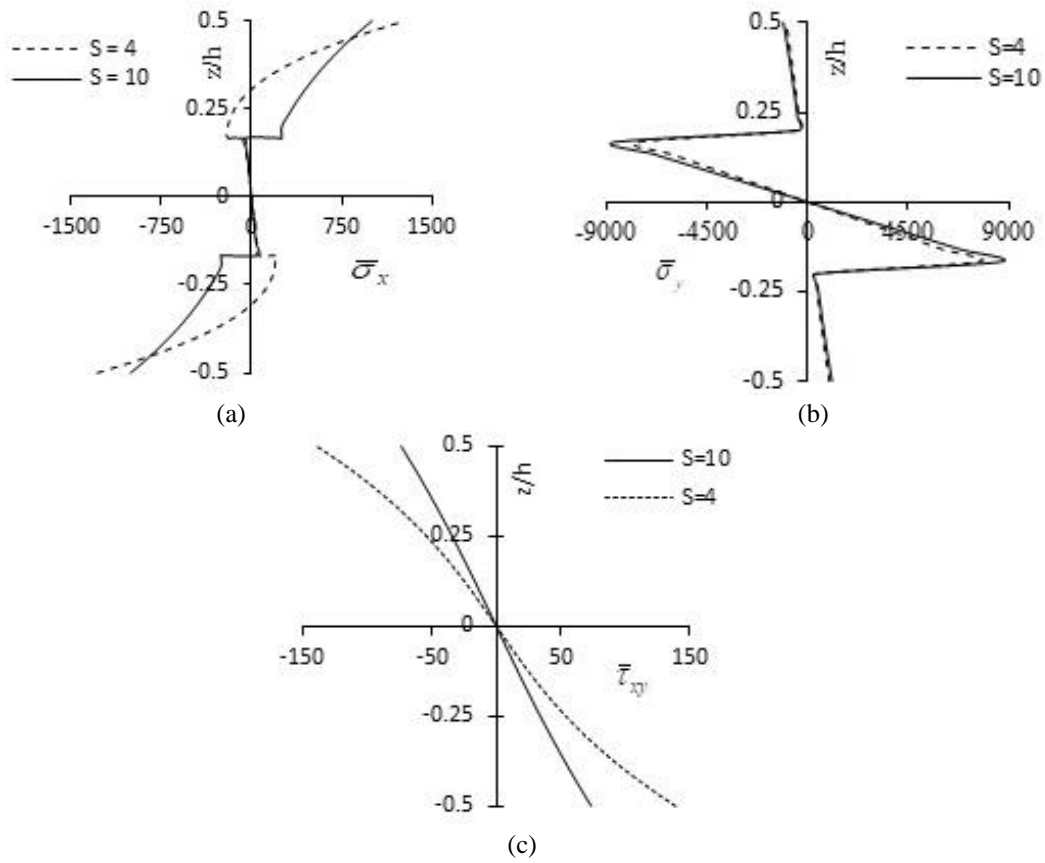


Fig. 12 Variation of normalized inplane stresses ( $\bar{\sigma}_x, \bar{\sigma}_y$ ) and inplane shear stresses ( $\bar{\tau}_{xy}$ ) through the thickness of three layer ( $0^0/90^0/0^0$ ) laminated plate subjected to single sinusoidal linear thermal load for aspect ratios 4 and 10

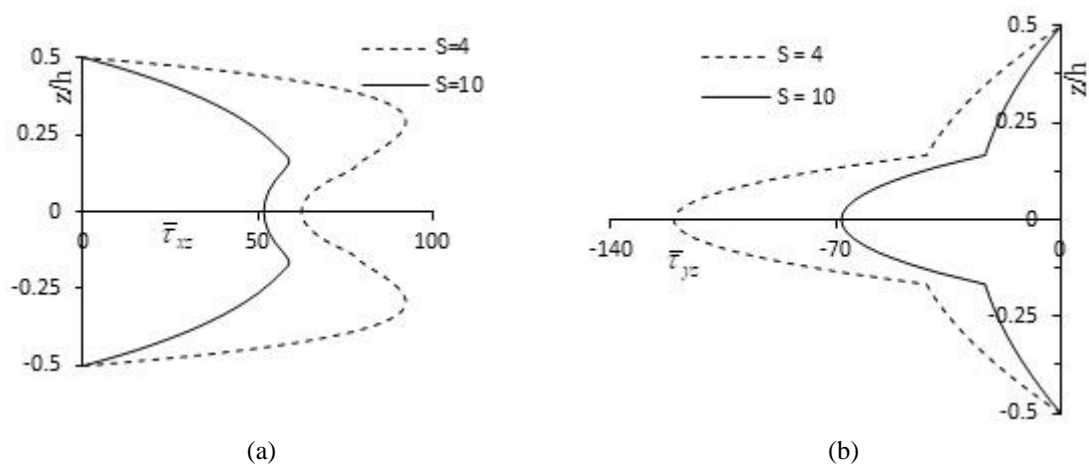


Fig. 13 Variation of normalized transverse shear stresses ( $\bar{\tau}_{xz}, \bar{\tau}_{yz}$ ) through the thickness of three layer ( $0^0/90^0/0^0$ ) laminated plate subjected to single sinusoidal linear thermal load for aspect ratios 4 and 10

plate due to shear and normal deformation effects subjected to linear sinusoidal thermal load for aspect ratio 4, whereas variation of displacement  $\bar{v}$  is linear across thickness of plate.

It is observed from the results that the transverse displacements ( $\bar{w}$ ) obtained by present theory, HSDT and exact theory are in excellent agreement with each other for all the aspect ratios due to inclusion of transverse normal strain effect in these theories. However, FSDT and CPT underpredict the values for aspect ratios 10 and 20.

The present theory predicts higher values of inplane normal stresses  $\bar{\sigma}_x$  and  $\bar{\sigma}_y$  for aspect ratio 4 as compared to the results of HSDT and exact theory. For aspect ratios 10, 20, and 50 results of these stresses by present theory, HSDT, FSDT and CPT are in good agreement with those of exact theory. Present theory underpredicts the value of inplane shear stress for aspect ratio 4 and predicts very good values for aspect ratios 10, 20, and 50 compared to the results of HSDT and exact theory. The through thickness variations of inplane stresses is shown in Fig. 12 for aspect ratios 4 and 10. The variations of  $\bar{\sigma}_x$  and  $\bar{\tau}_{xy}$  across the thickness of laminated plate are nonlinear for thick plate ( $S = 4$ ) due to significant shear and thickness stretching effects when subjected to linear sinusoidal thermal load, whereas that of  $\bar{\sigma}_y$  is layerwise linear due to reversal of stacking sequence in that direction.

Transverse shear stresses ( $\bar{\tau}_{xz}, \bar{\tau}_{yz}$ ) obtained by present theory are in excellent agreement with those HSDT and exact theory for all the aspect ratios. FSDT and CPT overpredict the values of these stresses for aspect ratio 10 and yield excellent values for aspect ratios 20 and 50 as compared to the results of exact theory. The through the thickness variations of transverse shear stresses are shown in Fig. 13. The variation of transverse shear stress across the thickness of laminated plate satisfies the continuity condition at the interfaces between the layers and the stress free conditions on the top and bottom surfaces of the plate.

It is observed from above discussion that the transverse normal deformation or thickness stretching effect has the significant on the improvement of thermoelastic response symmetric cross-ply laminated plates subjected to linear thermal load.

## 5. Conclusions

In this study, thermal stress analysis of orthotropic, antisymmetric and symmetric cross-ply laminated plates subjected to single sinusoidal linear and nonlinear thermal loads across the thickness of plate is presented based on trigonometric shear and normal deformation theory. The thickness stretching effect is included for more accurate analysis. The displacement field is built upon the classical plate theory using trigonometric functions in terms of thickness coordinate to include both the transverse shear and normal deformation effects. The principle virtual work is used to derive the governing equations and boundary conditions. Thermoelastic displacements and stresses for simply supported plates are obtained using Navier's solution technique and compared with the results of other refined theories disregarding thickness stretching effect. Following conclusions are drawn from the results and discussion.

1. The results of displacements and stresses obtained by present theory deviate considerably for thick orthotropic and antisymmetric cross-ply laminated plates as compared to those of other refined theories due to the neglect of thickness stretching effect in other theories while subjecting

the plates to nonlinear thermal load.

2. The present theory is in excellent agreement with exact theory while predicting the thermal response of symmetric cross-ply laminated plate under linear thermal load and agrees well with other refined theories for symmetric crossply plates under nonlinear thermal load.

3. The numerical results indicate that the effect of thickness stretching is more important in predicting more accurate transverse shear stresses or interlaminar stresses across the thickness of laminated plates.

Therefore, it can be concluded that the effect of transverse normal deformation or thickness stretching effect is inevitable while performing the thermal stress analysis of laminated composite plates subjected to linear and nonlinear thermal loads.

## References

- Altay, G.A. and Doekmeci, M.Q. (2003), "Some comments on the higher-order theories of piezoelectric, piezothermoelectric, and thermopiezoelectric rods and shells", *Int. J. Solids Struct.*, **40**(18), 4699-4706. [https://doi.org/10.1016/S0020-7683\(03\)00185-9](https://doi.org/10.1016/S0020-7683(03)00185-9).
- Arefi, M. and Amabili, M. (2021), "A comprehensive electro-magneto-elastic buckling and bending analyses of three-layered doubly curved nanoshell, based on nonlocal three-dimensional theory", *Compos. Struct.*, **257**(1), 113101+18. <https://doi.org/10.1016/j.compstruct.2020.113100>.
- Arefi, M. and Arani, A.H.S. (2020), "Nonlocal vibration analysis of the three-layered FG nanoplates subjected to applied electric potential considering thickness stretching effect", *Proc. Inst. Mech. E Part L J. Mat. Des. Appl.*, **234**(9), 1183-1202. <https://doi.org/10.1177/1464420720928378>.
- Arefi, M. and Zenkour, A.M. (2016), "A simplified shear and normal deformations nonlocal theory for bending of functionally graded piezomagnetic sandwich nanobeams in magneto-thermo-electric environment", *J. Sandw. Struct. Mater.*, **18**(5), 1-28. <https://doi.org/10.1177/1099636216652581>.
- Arefi, M. and Zenkour, A.M. (2018), "Free vibration analysis of a three-layered microbeam based on strain gradient theory and three-unknown shear and normal deformation theory", *Steel Compos. Struct.*, **26**(4), 421-437. <http://doi.org/10.12989/scs.2018.26.4.421>.
- Arefi, M., Bidgoli, E.M.R. and Civalek, O. (2020), "Bending response of FG composite doubly curved nanoshells with thickness stretching via higher-order sinusoidal shear theory", *Mech. Based Des. Struct. Mach.*, **1**, 1-29. <http://doi.org/10.1080/15397734.2020.1777157>.
- Bhaskar, K., Varadan, T.K. and Ali, J.S.M. (1996), "Thermoelastic solutions for orthotropic and anisotropic composite laminates", *Compos. Part B*, **27**(5), 415-420. [https://doi.org/10.1016/1359-8368\(96\)00005-4](https://doi.org/10.1016/1359-8368(96)00005-4).
- Carrera, E. (2000), "An assessment of mixed and classical theories for the thermal stress analysis of orthotropic multi-layered plates", *J. Therm. Stresses*, **23**(9), 797-831. <https://doi.org/10.1080/014957300750040096>.
- Carrera, E. and Ciuffreda, A. (2004), "Closed-form solutions to assess multilayered plate theories for various thermal stress problems", *J. Therm. Stresses*, **27**(11), 1001-1031. <https://doi.org/10.1080/01495730490498584>.
- Carrera, E. (2005), "Transverse normal strain effects on thermal stress analysis of homogeneous and layered plates", *AIAA J.*, **43**(10), 2232-2242. <https://doi.org/10.2514/1.11230>.
- Carrera, E., Cinefra, M. and Fazzolari, F.A. (2013), "Some results on thermal stress by using unified formulation for plates and shells", *J. Therm. Stresses*, **36**(6), 589-625. <https://doi.org/10.1080/01495739.2013.784122>.
- Cho, K.N., Striz, A.G. and Bert, C.W. (1989), "Thermal stress analysis of laminate using higher-order theory in each layer", *J. Therm. Stresses*, **12**(3), 321-332. <https://doi.org/10.1080/01495738908961970>.
- Dehsaraji M.L., Arefi M. and Loghman A. (2020), "Three dimensional free vibration analysis of functionally graded nano cylindrical shell considering thickness stretching effect", *Steel Compos. Struct.*, **34**(5), 657-

670. <http://doi.org/10.12989/scs.2020.34.5.657>.
- Dehsaraji, M.L., Arefi, M. and Loghman, A. (2021), "Size dependent free vibration analysis of functionally graded piezoelectric micro/nano shell based on modified couple stress theory with considering thickness stretching effect", *Defence Tech.*, **17**(1), 119-134. <https://doi.org/10.1016/j.dt.2020.01.001>.
- Dehsaraji, M.L., Arefi, M. and Loghman, A. (2021), "Thermo electro-mechanical buckling of FGP nano shell with considering thickness stretching effect based on size dependent analysis", *Mech. Based Des. Struct. Mach.*, 1-22. <https://doi.org/10.1080/15397734.2021.1873146>.
- Fares, M.E., Zenkour, A.M. and El-Marghany, M.Kh. (2000), "Non-linear thermal effects on the bending response of cross-ply laminated plates using refined first-order theory", *Compos. Struct.*, **49**(3), 257-267. [https://doi.org/10.1016/S0263-8223\(99\)00137-3](https://doi.org/10.1016/S0263-8223(99)00137-3).
- Ghugal, Y.M. and Shimpi, R.P. (2002), "A review of refined shear deformation theories of isotropic and anisotropic laminated plates", *J. Reinf. Plast. Compos.*, **21**(9), 775-811. <https://doi.org/10.1177/073168402128988481>.
- Ghugal, Y.M. and Kulkarni, S.K. (2011), "Thermal stress analysis of cross-ply laminated plates using refined shear deformation theory", *J. Exp. App. Mech.*, **2**(1), 47-66.
- Ghugal, Y.M. and Kulkarni, S.K. (2013), "Thermal flexural analysis of cross-ply laminated plates using trigonometric shear deformation theory", *Lat. Amer. J. Solids Struct.*, **10**(5), 1001-1023.
- Ghugal, Y.M. and Kulkarni, S.K. (2012), "Effect of aspect ratio on transverse displacements for orthotropic and two layer laminated plates subjected to non-linear thermal loads and mechanical loads", *Int. J. Civ. Struct. Eng.*, **3**(1), 186-196.
- Ghugal, Y.M. and Kulkarni, S.K. (2013), "Flexural analysis of cross-ply laminated plates subjected to nonlinear thermal and mechanical loadings", *Acta Mech.*, **224**(3), 675-690. <https://doi.org/10.1007/s00707-012-0774-1>.
- Jane, K.C. and Hong, C.C. (2000), "Thermal bending analysis of laminated orthotropic plates by the generalized differential quadrature method", *Mech. Res. Commun.*, **27**(2), 157-164. [https://doi.org/10.1016/S0093-6413\(00\)00076-8](https://doi.org/10.1016/S0093-6413(00)00076-8).
- Kapania, R.K. and Mohan, P. (1996), "Static, free vibration and thermal analysis of composite plates and shells using a flat triangular shell element", *Comput. Mech.*, **17**, 343-357. <https://doi.org/10.1007/BF00368557>.
- Khare, R.K., Kant, T. and Garg, A.K. (2003), "Closed-form thermo-mechanical solutions of higher-order theories of cross-ply laminated shells", *Compos. Struct.*, **59**(3), 313-340. [https://doi.org/10.1016/S0263-8223\(02\)00245-3](https://doi.org/10.1016/S0263-8223(02)00245-3).
- Khdeir, A.A. and Reddy, J.N. (1991), "Thermal stresses and deflections of cross-ply laminated plates using refined plate theories", *J. Therm. Stresses*, **14**(4), 419-438. <https://doi.org/10.1080/01495739108927077>.
- Kirchhoff, G. (1850), "Über das gleichgewicht und die bewegung einer elastischen scheinbe", *J. für die Reine und Angew. Math.*, **40**, 51-88. <https://doi.org/10.1515/crll.1850.40.51>.
- Matsunaga, H. (1992), "The application of a two-dimensional higher-order theory for the analysis of a thick elastic plate", *Comput. Struct.*, **45**(4), 633-648. [https://doi.org/10.1016/0045-7949\(92\)90482-F](https://doi.org/10.1016/0045-7949(92)90482-F).
- Matsunaga, H. (2002), "Assessment of a global higher-order deformation theory for laminated composite and sandwich plates", *Compos. Struct.*, **56**(3), 279-291. [https://doi.org/10.1016/S0263-8223\(02\)00013-2](https://doi.org/10.1016/S0263-8223(02)00013-2).
- Matsunaga, H. (2003), "Interlaminar stress analysis of laminated composite and sandwich circular arches subjected to thermal/mechanical loading", *Compos. Struct.*, **60**(3), 345-358. [https://doi.org/10.1016/S0263-8223\(02\)00340-9](https://doi.org/10.1016/S0263-8223(02)00340-9).
- Matsunaga H. (2004), "A Comparison between 2-D single-layer and 3-D layerwise theories for computing interlaminar stresses of laminated composite and sandwich plates subjected to thermal loadings", *Compos. Struct.*, **64**(2), 161-177. <https://doi.org/10.1016/j.compstruct.2003.08.001>.
- Matsunaga, H. (2005), "Thermal buckling of cross-ply laminated composite and sandwich plates according to a global higher-order deformation theory", *Compos. Struct.*, **68**(4), 439-454. <https://doi.org/10.1016/j.compstruct.2004.04.010>.
- Matsunaga, H. (2006), "Thermal buckling of angle-ply laminated composite and sandwich plates according to a global higher-order deformation theory", *Compos. Struct.*, **72**(2), 177-192.

- <https://doi.org/10.1016/j.compstruct.2004.11.016>.
- Matsunaga, H. (2007a), "Free vibration and stability of angle-ply laminated composite and sandwich plates under thermal loading", *Compos. Struct.*, **77**(2), 249-262.  
<https://doi.org/10.1016/j.compstruct.2005.07.002>.
- Matsunaga, H. (2007b), "Thermal buckling of cross-ply laminated composite shallow shells according to a global higher-order deformation theory", *Compos. Struct.*, **81**(2), 210-221.  
<https://doi.org/10.1016/j.compstruct.2006.08.008>.
- Mindlin, R.D. (1951), "Influence of rotatory inertia and shear on flexural motions of isotropic, elastic plates", *J. Appl. Mech.*, **18**(1), 31-38. <https://doi.org/10.1115/1.4010217>.
- Nguyen, T.N., Thai, C.H. and Xuan, H.N. (2016), "On the general framework of high order deformation theories for laminated composite plate structures: A novel unified approach", *Int. J. Mech. Sci.*, **110**, 242-255. <https://doi.org/10.1016/j.ijmecsci.2016.01.012>.
- Noor, A.K. and Burton, W.S. (1989), "Assessment of shear deformation theories for multilayered composite plates", *Appl. Mech. Rev.*, **42**(1), 1-13. <https://doi.org/10.1115/1.3152418>.
- Noor, A.K. and Burton, W.S. (1990), "Assessment of computational models for multilayered anisotropic plates", *Compos. Struct.*, **14**(3), 233-265. [https://doi.org/10.1016/0263-8223\(90\)90050-O](https://doi.org/10.1016/0263-8223(90)90050-O).
- Noor, A.K. and Burton, W.S. (1992), "Computational models for high- temperature multi-layered composite plates and shells", *Appl. Mech. Rev.*, **45**(10), 419-446. <https://doi.org/10.1115/1.3119742>.
- Reddy, J.N. (1984), "A simple higher-order theory for laminated composite plates", *J. App. Mech.*, **51**(4), 745-752. <https://doi.org/10.1115/1.3167719>.
- Reddy, J.N. (1993), "An evaluation of equivalent single layer and layerwise theories of composite laminates", *Comput. Struct.*, **25**(1-4), 21-35. [https://doi.org/10.1016/0263-8223\(93\)90147-I](https://doi.org/10.1016/0263-8223(93)90147-I).
- Vekua, I.N. (1985), *Shell Theory: General Methods of Construction*, Pitman Advanced Publishing Program, Boston, U.S.A.
- Yokoo, Y., and Matsunaga, H. (1974), "A general nonlinear theory of elastic shells", *Int. J. Solids Struct.*, **10**(2), 261-274. [https://doi.org/10.1016/0020-7683\(74\)90023-7](https://doi.org/10.1016/0020-7683(74)90023-7).
- Zenkour, A.M. (2004), "Analytical solution for bending of cross-ply laminated plates under thermo-mechanical loading", *Compos. Struct.*, **65**(3-4), 367-379.  
<https://doi.org/10.1016/j.compstruct.2003.11.012>.
- Zhavoronok, S.A. (2014), "Vekua-type linear theory of thick elastic shells", *ZAMM J. Appl. Math. Mech.*, **94**(1-2), 164-184. <https://doi.org/10.1002/zamm.201200197>.
- Zozulya, V.V. (2013), "A high order theory for linear thermoelastic shells: Comparison with classical theories", *J. Eng.*, 1-19. <https://doi.org/10.1155/2013/590480>.
- Zozulya, V.V. (2015), "A higher order theory for shells, plates and rods", *Int. J. Mech. Sci.*, **103**, 40-54. <https://doi.org/10.1016/j.ijmecsci.2015.08.025>.